

## Microscopy at the Bottom

U. Kaiser, A. Chuvilin, J. Meyer, J. Biskupek

Central Facility for Electron Microscopy, Group of Materials Science Electron Microscopy,  
Albert Einstein Allee 11, 89081 Ulm.

ute.kaiser@uni-ulm.de

Keywords: High resolution TEM, aberration correction, resolution limit

About twenty years ago, many experts were still pessimistic about the possibility for making qualitative significant advancements in resolution improvement of the electron microscope. The basis for their scepticism was the Scherzer Theorem [1], which states that axially symmetric electromagnetic lenses have large intrinsic spherical and chromatic aberrations, limiting the resolution of an electron microscope to about 100 times the wavelength of the imaging electrons. This is exactly the situation to which Richard Feynman referred 50 years ago when writing: "It would be very easy to make an analysis of any complicated chemical substance; all one would have to do would be to look at it and see where the atoms are. The only trouble is that the electron microscope is one hundred times too poor" [2]. Feynman further stated that it should, however, not be impossible to improve the electron optic of the microscopes as "it is not against the law of diffraction of the electron. The wave length of the electron in such a microscope is only 1/20 of an angstrom. So it should be possible to see individual atoms. What good would it be to see the individual atoms distantly!"

Prior to Rose's designing the first non-axially symmetric lenses that actually could correct the aberrations inherent to round magnetic lenses [3], the instrumental resolution of TEMs was limited primarily by the spherical aberration ( $C_s$ ) of the objective lens and the wavelength of the electrons. Therefore, reduction of the wavelength was the only possibility for improving the resolution. However, because of the occurrence of radiation damage, high-voltage instruments could not be used for many applications as even thick crystalline materials can be observed under MeV beams only for a few minutes [4]. After the practical realization of the  $C_s$ -corrector for the TEM in 1998 [5] and STEM in 1999 [6] and its commercial premiere in 2005, atomic resolution of material's heavy and light single atom columns and even single heavy atoms at medium accelerating voltages has become a reality. An enormously huge wealth of materials science questions can now be addressed - and answered. Atom column dumbbells, which never were resolved so far can now be imaged distantly (see Fig. 1).

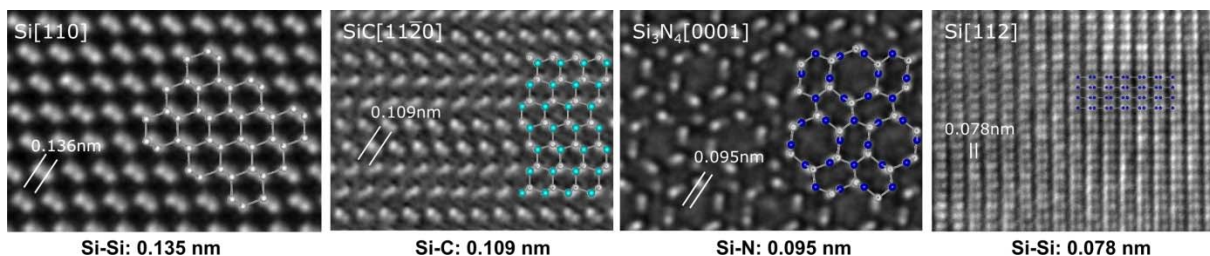


**Figure 1.** The figure show  $C_s$ -corrected HRTEM images taken at 300kV with small negative  $C_s$  and small positive defocus showing bright atom columns. The dumbbells of [110]Si, [11-20]4H-SiC, [0001]  $Si_3N_4$  and [112] Si can be resolved (the model of the structures are overlaid).

Optimum contrast conditions were found for high resolution imaging with spherical aberration corrected instruments at medium voltages, which are NCSI (negative  $C_s$  imaging

[7]) conditions - that means negative  $C_s$  and over-focus - resulting in ‘white-atom’ contrast on dark background, and they are especially useful for imaging weakly scattering light atoms in the surrounding of strongly scattering heavy atoms, for the case that the linear imaging theory can be applied [8, 9]. Since then, imaging with variable spherical aberration is a practical reality and single atomic columns with different atomic numbers adjacent to each other can be imaged both in aberration corrected imaging and scanning TEM mode [10, 11, 12, 13, 14, 15]. In high resolution optimal imaging conditions change for thick specimens, where the contribution of amplitude contrast cannot be neglected [16,11]. In future, very exact tuning of the  $C_s$  coefficient may allow pure phase contrast imaging of the exit wave if the weak phase object approximation is fulfilled, as demonstrated for the case of  $Si_3N_4$  [11].

In the ideal case of a radiation-resistant specimen, the resolution of the image is determined only by the instrumental resolution and therefore the increase of accelerating voltage will give highest resolution. However, real samples are always damaged by the electron beam and thus by the tolerable duration for observation. For many materials science questions, medium voltages are, nevertheless, most often used mainly for three reasons: (1) for a number of materials, knock-on damage can be tolerated within shorter observation time and the gain in resolutions is motivating the electron energy, (2) the preparation of very thin samples required when decreasing the acceleration voltages is not yet developed appropriately, and/or (3) the application requires thicker samples.

The achievable resolution in the final high resolution experiment becomes a function not only of the instrumental but also of the specimen resolution limit. The latter is determined by the time of observation or in other words by the tolerable dose, the contrast and the S/N [17]. The maximum tolerable dose depends on physical processes occurring due to interaction of the incident electrons with the atoms of the sample. The most important effects are knock-on damage, ionisation, heating, and chemical etching due to residual molecules in vacuum.

Many carbon materials will be immediately destroyed by knock-on damage when imaging at 300kV. As seen in Fig. 2, these carbon nanotubes (CNT) can be imaged undestroyed only at 80kV; please note the strong increase in contrast at lower voltage [18] and the atomic resolution reachable only with the spherical aberration corrected technology (see Figs 2 and 3).

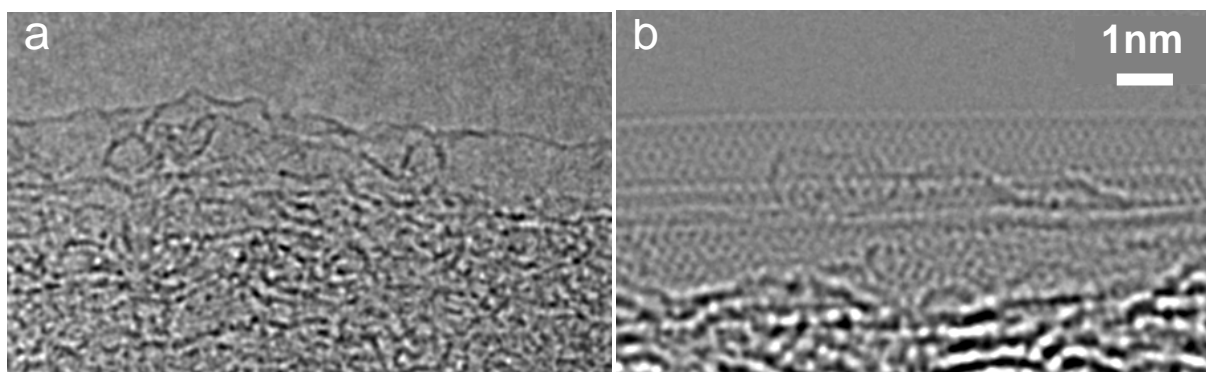


**Figure 2.** SWNT imaged in HRTEM on carbon soot (a) after 10 sec electron irradiation at 300 kV (b) after 20 min electron irradiation at 80 kV. In (b) the lattice is clearly resolved. Compare the contrast of carbon soot in both images.

As state-of-the-art aberration corrected TEMs can be operated also at 80kV, therefore 80keV electrons are used for imaging carbon materials at sufficient high resolution for imaging single carbon “atoms distantly” in nanocarbon materials [19, 20]. As in Fig. 2a, surface knock-on damage is the dominant radiation damage mechanism, because the fraction

of surface atoms is very high for such systems. The threshold energy for surface-atom knock-on is much lower than that for atoms in the bulk (e.g. graphite 140 kV [21] and C in CNT <90 kV [22]) and ranges between 20-80kV for low  $Z$ -number surface atoms [23]. Knock-on damage decreases with lower voltage, however the other important radiation damage mechanisms, heating, ionization, and chemical etching are increasing mainly because the inelastic cross-section increases with decreasing voltage. It should be noted that the latter fact results in an increase of the inelastic signals, which is of strong advantage for EDS and EELS experiments.

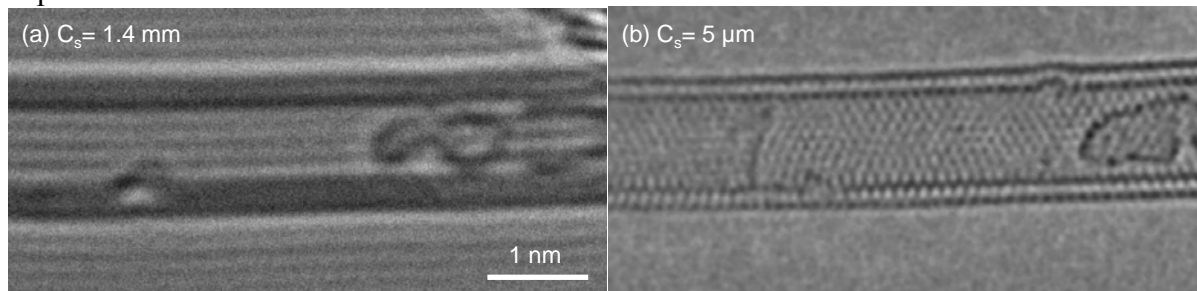


**Figure 3.** 80kV HRTEM image of a double walled CNT imaged (a) without the correction of the spherical aberration and (b) with correction.

With particular care or in certain cases, ionization and heating might be significantly reducible. Ionization, which occurs when the incident electrons eject valence electrons from the sample, can be reduced in the case of carbon materials having delocalized  $\pi$ -electrons, a vacancy can be refilled in a few femto-seconds, before bonds will break. For organic molecules with sigma-bonds and for insulating crystals, this is more complicated. Approaches to reduce ionisation damage exist already, which are e.g. inserting the molecules into carbon nanotubes before imaging [24]. In addition, as this may not always work because of the limited size for the CNT, it might be possible to sandwich the beam sensitive material just in-between two graphene sheets.

Damage of the sample because of increase in temperature during observation has strongly to be taken into account for carbon materials with sigma bonds: heating up to more than 100°C may occur locally depending on the thermal conductivity of the material. It can be effectively reduced by using a cooling holder.

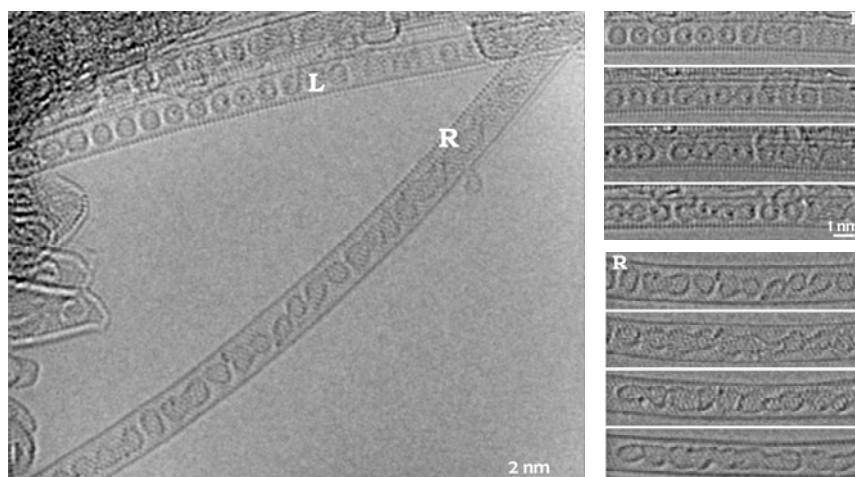


**Figure 4** (from reference [25]): 80kV HRTEM image of endohedral Dy atoms inside fullerenes filled in SWNT. Atoms are black. The difference in the coalescence of fullerenes in two adjacent nanotubes, one of which (right) is wider and free standing and the other (left) is narrower and is in a good contact with the sample grid both thermally and electrically. Both nanotubes (L and R) are exposed to the same dose. It is clearly seen from the time sequence (from the top 1, 3, 6, 8min, respectively) that coalescence of the fullerenes is significantly inhibited in the left nanotube (marked L).

For a fixed dose of incident electrons heating will increase with decreasing accelerating voltage. For materials such as graphene and carbon nanotubes, this effect is neglectable because they are excellent heat conductor under the presumption that they have good contact with the TEM grid (Fig. 4). As can be seen, the endohedral fullerenes inside the left nanotube (marked L), which has good contact to the TEM grid, are stable for much longer time than in the right (marked R) nanotube, where a double walled CNT has been formed out of the fullerenes already after about 8min of observation.

Another important origin of beam damage is chemical etching and it is assumed that the water content in the vacuum mainly determines the etching rate [26]. Therefore the ice contamination rate had been determined for our instrument. To which extent other species contribute, will be a matter of further investigation.

In the following, two experiments on single-layer graphene have been selected showing the capability of existing state-of-the-art 80kV spherical aberration corrected technology for observing and manipulating single carbon atoms performed in a FEI-TITAN 80-300. Such characterization we regarded as a first step. In a second step, which is our final aim, graphene will be used as low noise substrate for imaging beam sensitive materials where, after subtraction from the graphene matrix, the agglomerates can be imaged as if they were freestanding in vacuum. However, this will require even lower voltages and higher resolution than is currently possible.

Fig. 5 shows a 80kV high-resolution image of single-layer graphene, where about 10 atoms were knocked-out due to our short irradiation with a dose of  $10^7$  e-/nm<sup>2</sup> at 300kV. It is interesting to note that after reconstruction all carbon atoms remain in planar sp<sup>2</sup> type configuration, which is rather stable in clean specimen areas. These or other artificially created defects might serve as preferred places for low contrast adsorbates in the future.

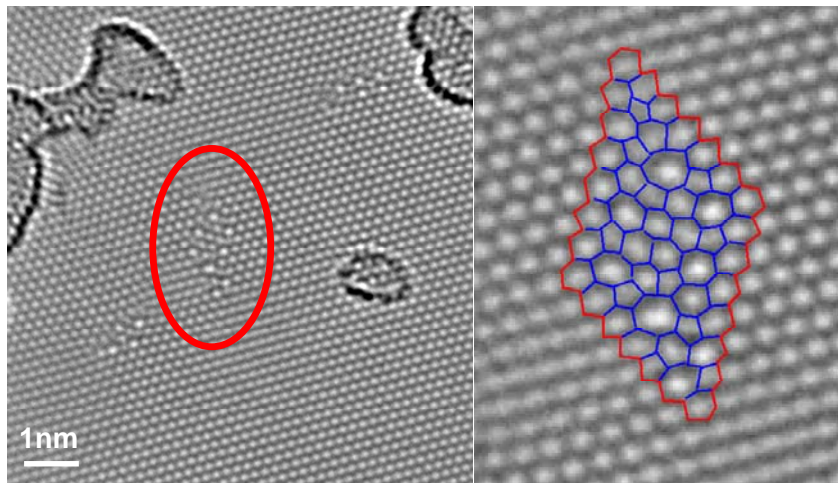


**Figure 5.** 80kV HRTEM image of the effect of knock-on damage in graphene created after very brief irradiation at 300kV ( $10^7$  e-/nm<sup>2</sup>). Atoms are dark. (right): Higher magnification of the encircled area on the left. It is seen that the defects are not simple vacancies; ca. 1nm-sized area is reconstructed around 10 atoms, knocked out compared to the ideal lattice.

State of the art graphene preparation [27] still does not allow to receive perfectly clean substrate. Contamination always is present and exactly this is the preferred place, where holes start to grow. In-between two holes, graphene ribbons and after a certain time, single carbon atom chains form, as can be seen in Fig. 6. These chains were surprisingly stable under the electron beam. So far all observed chains did not show indication of a zig-zag structure, therefore one of the two possible linear configurations, either the cumulene or poly-yne type

[28] we suppose to exist. Calculations showed that it depends on the number of carbon atoms (even or odd) which model exist [28], however in our experiment, the signal to noise ratio was not sufficient to reliably count the carbon atoms in the chains.

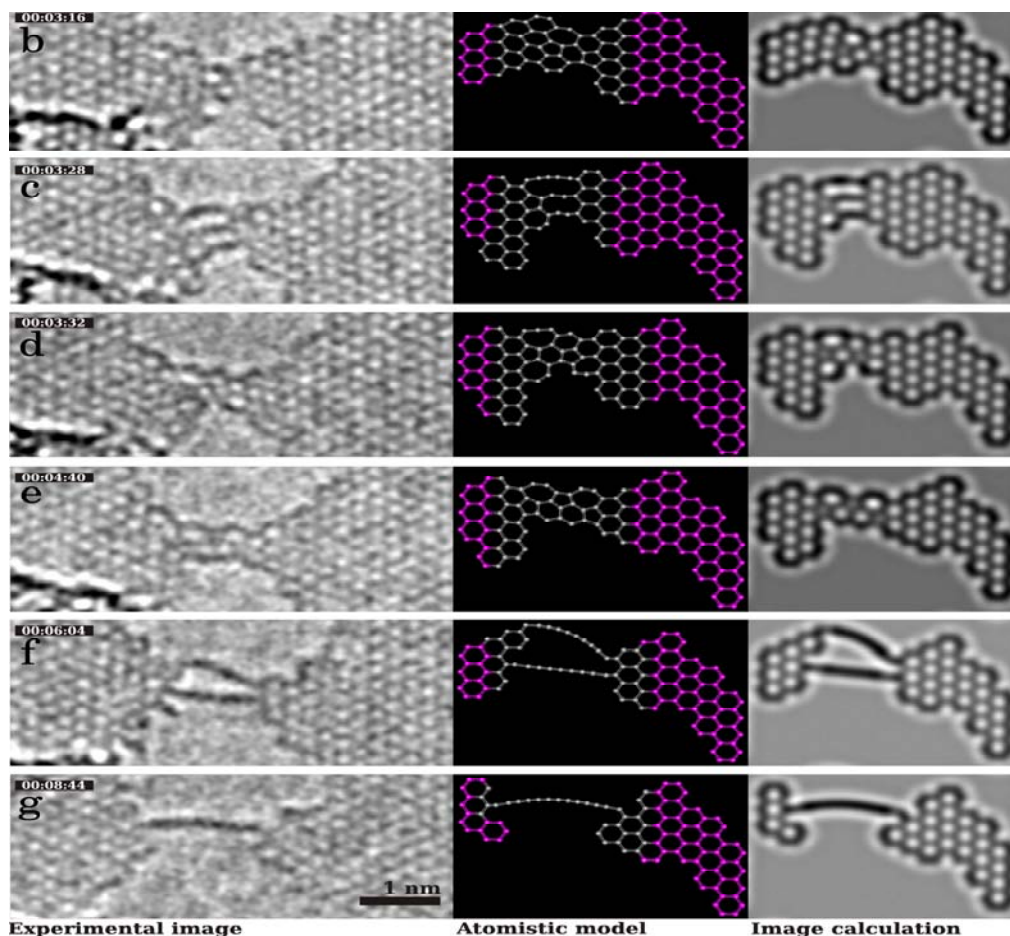


**Figure 6** (from reference [29]): 80kV HRTEM images of the transition from a graphene ribbon in-between two holes to a single carbon chain. Atoms are dark (b-g) Time evolution of the bridge, in the experimental image (left), atomistic model (center), and corresponding image calculation (right). Carbon chains are present in panels (c, f, g); reconstructed bridge configurations of planar covalent carbon networks are seen in (b, d, e).

To conclude: There is a wealth of interesting physical phenomena related to radiation damage in graphene and related materials [30] to be studied and understood before it will serve as a clean low noise platform for further experiments with beam sensitive materials on top or in-between two graphene sheets. As materials need to be imaged below their surface knock-on damage threshold, there is a demand for low voltage electron microscopy. At low voltages in particular it is not enough to correct for  $C_S$ , as the chromatic aberration ( $C_C$ ) of the objective lens is strongly limiting the resolution. As a hexapole-corrector cannot correct for  $C_C$ , a new design—consisting of symmetrical multipole-quintuplets—that enables the correction of  $C_S$  and  $C_C$  without inducing higher-order aberrations, needs to be implemented [31, 32]. Such development will be beneficial for the following group of materials:

- (1) Electrically and thermally conducting solid materials, such as metals and nanocarbons
- (2) For insulators and organic materials, two properties are in competition when going to lower voltages: (a) the increase in ionization damage and (b) the increase in contrast. It is experimentally shown [33] that with decreasing HT, contrast is increasing faster than damage, thus S/N should be improved at low voltage.

In summary, the beneficial features of low-voltage TEM are the elimination of knock-on damage and the increase of contrast, S/N and increase of inelastic signals (EDS, EELS) Owing to these advantages the required dose decreases to such an extent that the deleterious effects caused by the increase of ionization and heating damage may be reduced<sup>34</sup>.

1. O. Scherzer, *Z- Phys.* **101** (1936) p593.
2. R. Feynman, Lecture 29<sup>th</sup>, 1959, on the annual meeting of the American Physical Society
3. H. Rose *Optik* **85** (1990) p19.
4. G. Dehm, K. Nadarzynski, F. Ernst, M. Rühle, *Ultramicroscopy* **63** (1996) p49.
5. M. Haider, S. Uhlemann, E. Schwan, H. Rose, B. Kabius, and K. Urban, *Nature* **392** (1998) p768
6. O. L. Krivanek, N. Dellby, and A. R. Lupini, *Ultramicroscopy* **78** (1999) p1.
7. C.L. Jia, M. Lentzen, K. Urban, *Science*, **299** (2003) p870.
8. M. Lentzen, B. Jahnen, C.L. Jia, A. Thust, K. Tillmann, K. Urban, *Ultramicroscopy*, **92** (2002) p233
9. C.L. Jia, M. Lentzen, K. Urban. *Microsc. Microanal.* **10** (2004) p174
10. K. W. Urban: *Science*, 321, 5888 (2008) p. 506.
11. Z. Zhang and U. Kaiser *Ultramicroscopy* (2009), DOI.10.1016.ultramic.2009.04.004.
12. D. Muller, M. Bosman et al., *Phys. Rev. Lett.* **99** (2007) p086102
13. Z. L. Zhang, U. Kaiser, S. Soltan, H-U. Habermeyer, B. Keimer (2009) submitted
14. J. E. Allen, E. R. Hemesath, D. E. Perea, J. L. Lensch-Falk, Z.Y. Li, F. Yin, M. H. Gass, P. Wang, A. L. Bleloch, R. E. Palmer, L. J. Lauhon, *Nature Nanotech.* **3**, (2008) p168
15. D. A. Muller, L. Fitting Kourkoutis, M. Murfitt, J. H. Song, H. Y. Hwang, J. Silcox, N. Dellby, O. L. Krivanek *Science* **319**, (2008) p1073.
16. M. Lentzen. *Ultramicroscopy* **99** (2004) p211.
17. H. Rose, *Microscopy and Microanalysis* **13** (2007) p134.
18. M. Malac, B. Beleggia, R. Egerton, Y. Zhu, *Ultramicroscopy* **107** (2007) 40.
19. J. C. Meyer, C. Kisielowski, R. Erni, M. D. Rossell, M. F. Crommie, and A. Zettl. *Nano Lett.*, **8** (2008) p3582.
20. J. H. Warner, Y. Ito, M. H. Rummeli, Th. Gemming, B. Büchner, H. Shinohara, G. A. D. Briggs, *Phys. Rev. Lett.* (2009) accepted
21. R.F. Egerton, P. Li, M. Malac, *Micron*, **35** (2004) p399.
22. A. Zobelli, A. Gloter, C. P. Ewels, G. Seifert, and C. Colliex, *Phys. Rev.B*, **75** (2007) p245402.
23. L.W Hobbs, In: Hren, J.J., Goldstein, J.I., Joy, D.C. (Eds.), Plenum Press, N. Y. (1987) p399.
24. Z. Lui, K. Yanagi, K. Suenaga, H. Kataura, S. Iijima, *Nature Nanotechnol.* **2**, (2007) p422
25. A. Chuvilin, A. N. Khlobystov, D. Obergfell, M. Haluska, S. Yang, S. Roth and U. Kaiser (2009) submitted
26. K. Molhave, S.B. Gudnason, A.T. Pedersen, C.H. Clausen, A. Horsewell, B. Boggild, *Ultramicroscopy* **103** (2007) p001.
27. J.C. Meyer, C.O. Girit, M. F. Crommie, A. Zettl, *Appl. Phys. Lett.* **92** (2008) p123110.
28. V. P. Bodart, J. Delhalle, M. Dory, J. G. Fripiat, and J.-M. Andre. *J. Opt. Soc. Am. B*, **4** (1987) p1047.
29. A. Chuvilin, J. C. Meyer, G. Algara-Siller, U. Kaiser, *New J. of Physics* (2009) accepted
30. J.C. Meyer, A. Chuvilin, G. Algara-Siller, J. Biskupek, U. Kaiser, *Nanoletter*, **9** (7) (2009) p2683.
31. H. Rose, *Nuc. Instr. Meth. Phys. Res. A* **519** (2004) p12.
32. M. Haider, *Ultramicroscopy* **108**, 3(2008) p167.
33. M.T. Hayashida, T. Kawasaki, Y. Kimura, Y. Takai, *Nuc. Instr. Phys. Res* **248** (2006) p273.
34. This work has been performed in the frame of the SALVE Projects KA1295/10-1,11-1 we acknowledge the support by the DFG and the State Baden Württemberg. We are grateful to Harald Rose for support and discussion.